Biomedical x-ray imaging with fluorescent and interferometric phase contrast method

Tohoru Takeda, *Akio Yoneyama, Jin Wu, Tsutomu Zeniya, Yoshinori Tsuchiya, Thet-Thet-Lwin, DV Rao, Shounosuke Matsushita, **Tetsuya Yuasa, Toru Yashiro, Yuji Aiyoshi, ***Kazuyuki Hyodo, ***Keiichi Hirano, ****Atsusi Momose, **Takao Akatsuka, Yuji Itai

Institute of Clinical Medicine, University of Tsukuba. Tsukuba-shi, Ibaraki 305-8575, Japan
*Advanced Research Laboratory, Hitachi, Ltd., Hatoyama, Saitama, 350-0395, Japan.
**Faculty of Engineering, Yamagata University. Yonezawa-shi, Yamagata 992-8510, Japan
***High Energy Accelerator Research Organization, Tsukuba-shi, Ibaraki 305-0801, Japan
****Department of Applied Physics, School of Engineering, University of Tokyo, Bunkyo-ku, Tokyo 113-8656, Japan

ABSTRACT

New types of synchrotron x-ray imaging such as fluorescent x-ray CT and phase-contrast x-ray imaging are being developed for biomedical research. While fluorescent x-ray CT (FXCT) can detect specific heavy atomic number elements at very low content (less than a few picogram iodine in a volume of 10^{-6} ml), the phase-contrast x-ray imaging is a highly sensitive imaging technique to differentiate the tissue in biological object. Therefore, with the high-contrast and high-spatial resolution, the functional information is revealed by FXCT and the morphological information is depicted by phase-contrast x-ray imaging.

Keywords: Synchrotron radiation, fluorescent x-ray CT, phase-contrast x-ray imaging, thyroid, tracer element, tumor

1. INTRODUCTION

Synchrotron radiation (SR) has several advantageous properties such as 1) the high photon flux density, 2) the broad energy spectrum, 3) the natural collimation and 4) the linear polarization. These properties of SR enable to develop new type of x-ray imaging techniques such as fluorescent and refraction phenomenon instead of the absorption-contrast method. Fluorescent x-ray CT detects very low contents of specific heavy atomic number elements, whereas the phase-contrast x-ray imaging depicts a minute difference within biological object composed by low atomic number elements [1-3]. In this article, we describe recent experimental results obtained by fluorescent x-ray CT and phase-contrast x-ray imaging.

Tohoru TAKEDA, MD, PhD

Institute of Clinical Medicine,
University of Tsukuba.
Tsukuba-shi, Ibaraki 305-8575 Japan
TeL:81-298-53-3774, Fax: 81-298-53-3658
E-mail: ttakeda@md.tsukuba.ac.jp

2. FLUORESCENT X-RAY CT

Fluorescent x-ray technique used in the planar mode is one of the most sensitive methods for detecting trace elements of medium or large atomic numbers [4]. It can evaluate very low contents in the order of picogram of elements. However, it requires the specimen to be cut into thin slices and to be scanned with a beam perpendicular to its surface. The FXCT method described here combines the sensitivity of fluorescence x ray with the cross-sectional capability of CT to detect very low content of elements for biomedical use. Especially the linear polarization of SR allows marked reduction of Compton scattering overlapped on the excited K_α fluorescent x-ray line and improves minimal detectability of elements.

Development of fluorescent x-ray tomography and computed tomography

Fluorescent x-ray tomography with SR was used to detect iron in the head of a bee in 1987 [5] and iodine in phantoms (200ng iodine in a volume of $4mm^3$) in 1995 [6,7]. However, in this tomographic method, the detection limit of excited fluorescent x-rays worsens as the requirement for higher spatial resolution. FXCT is highly efficient for detecting the excited fluorescent x-rays compared to the tomographic method because the FXCT system does not require intense collimation in detection site. FXCT was theoretically considered in 1991 [8], and could detect 60ng iodine in $1mm^3$ [9].

For the biomedical application, FXCT was first applied to depict the iodine distribution within thyroid gland at the spatial resolution of 1 mm [10,11], and now the thyroid gland [12] and rat myocardium labeled with non-radioactive iodine BMIPP [13] at less than 0.2mm spatial resolution. In ESRF, micro FXCT images with

0.006mm spatial resolution [14] was obtained.

Method and materials

FXCT system consists of a silicon (111) double crystal monochromator, a pin diode, an x-ray slit system, a scanning table for subject positioning, a fluorescent x-ray detector and a water cooled transmission x-ray CCD camera (Fig.1).

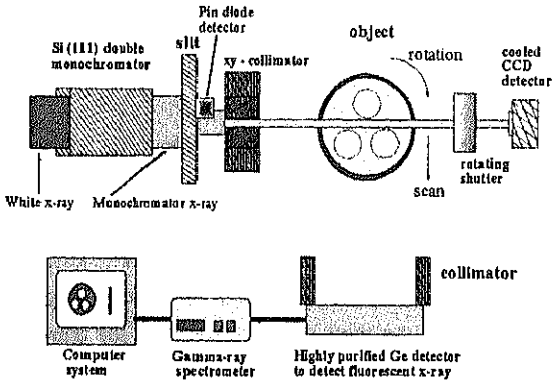

Fig.1 Schematic diagram of fluorescent x-ray CT

The fluorescent x-ray detector was positioned perpendicular to the incident monochromatic x-ray beam to reduce the scattered radiation. X-ray energy was set 37keV, and the incident monochromatic x ray was collimated into a 1x1mm to a 0.025x0.025mm pencil beam. Fluorescent x rays emitted isotropically from the subject along the path of the incident x-ray beam, were detected by a highly purity germanium detector [15,16].

The experiment was carried out at the bending-magnet beam line BLNE-5A of the Tristan accumulation ring (6.5GeV, 10-30mA) in Tsukuba, Japan. The photon flux before the object was $7x10^7$ photons/mm^2/s at a beam current of 30mA.

Image reconstruction

The net counts under the characteristic fluorescent K_α spectral lines at each projection were used to generate a CT image. The x-ray fluorescent data were corrected for the attenuation of the incident beam and the emitted fluorescent x-ray, using the attenuation information from the transmission x-ray CT image. Finally, the FXCT image was reconstructed by an algebraic method including the attenuation process [17].

Object

The objects were human thyroid tissues fixed in 10% formalin and rat myocardium labeled non-radioactive iodine BMIPP (metabolic agent of fatty acid). Phantom filled with iodine solution was obtained to achieve a quantitative estimation.

The present experiment was approved by the Medical Committee for the Use of Humans and Animals in Research of the University of Tsukuba.

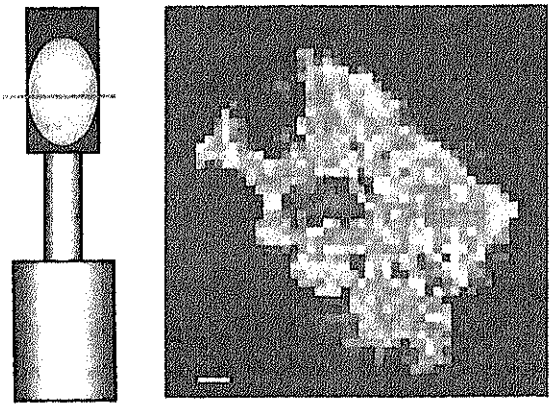

Fig.2 Fluorescent x-ray CT image of normal thyroid gland obtained at 0.05mm spatial resolution. Scale bar is 0.2mm.

Results and discussion

FXCT image of thyroid specimens

In normal thyroid, FXCT at 0.05mm spatial resolution depicted heterogeneous iodine distribution probably due to the inhomogeneous distribution of the iodine, vessel structures and connective tissues (Fig.2). However, transmission x-ray CT could not distinguish the inner structures due to the poor signal to noise ratio. In thyroid cancer, cancer specimen showed heterogeneous iodine distribution with small amount of iodine. Quantitative analysis revealed the concentration of iodine within cancer was less than 0.2mg/g. Thus, effectiveness of I-131 therapy might be predicted by FXCT because the accumulation dose of I-131 in thyroid cancer would be estimated.

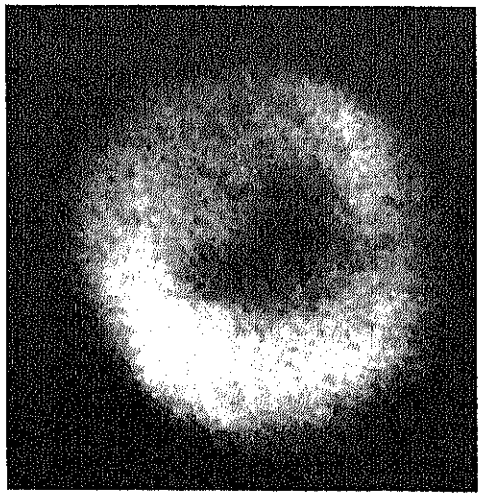

Fig.3 Fluorescent x-ray CT image of rat myocardium labeled with BMIPP. Diameter of heart is 10mm.

FXCT image of rat myocardium

FXCT image could clearly reveal the distribution of ^{127}I-BMIPP within myocardium at 0.1mm spatial resolution (Fig.3). The content of iodine in myocardium was estimated to be 0.01mg/g from the fluorescent K_α counts. Thus, FXCT will be used to evaluate the distribution of various labeling agents resembled to the autoradiogram.

3. PHASE-CONTRAST X-RAY IMAGING

Present clinical x-ray image is generated by the difference of linear attenuation coefficient within objects. However, the separation of biological structures such as cancer, fibrosis, necrosis and normal tissues is often difficult because the difference in the linear attenuation coefficients of these biological structures is very small.

Novel x-ray imaging technique named as phase-contrast x-ray imaging was developed using the wave nature of x ray. The sensitivity of this technique is about 1000times greater than that of absorption for low atomic-number elements such as hydrogen, carbon, nitrogen and oxygen [18] (Fig.4). For biological imaging, several phase-contrast x-ray imaging techniques such as an interferometric method [18-20] using a crystal x-ray interferometer [21], a Schlieren-like method using crystal diffraction [22,23], and a holography-like method [24-28] were developed. Among these methods, an interferometric method is the most sensitive method for detecting minute variation in soft tissue.

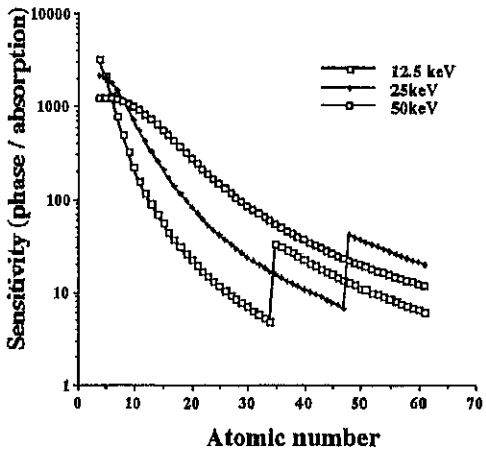

Fig.4 Sensitivity of phase contrast technique

Using an x-ray interferometer, phase-contrast x-ray radiography (phase map) clearly revealed cerebellar structures of a rat [18] and human metastatic tumor [19]. Phase-contrast x-ray CT [29] enabled to image inner structures of rabbit cancer [30], rat cerebrum [31] and human cancer [32,33]. However, the view size was limited less than 10mm due to the small size of interferometer. To image large object, new phase-contrast x-ray imaging system with a large monolithic x-ray interferometer and non-monolithic one is being developed. Here, present experimental results and possible future applications of this method are described.

Methods and Materials

The phase-contrast x-ray CT system consists of an asymmetrically cut silicon crystal, a monolithic x-ray interferometer having field of view 25x25mm [34], phase shifter, object cell and an x-ray CCD camera (Fig.5). The experiment was performed at a vertical wiggler beam line BL14C1 of the Photon Factory in Tsukuba, Japan. The typical beam current of the storage ring was 420mA at 2.5GeV ring energy. The x-ray energy was set at 17.7keV in the CT and vessel imaging and x-ray flux in front of the sample was estimated to be about $4x10^5$ photons/mm^2/s. Since the imaging at 35keV x-ray energy became possible from the last of 2001, the research of breast specimens has started.

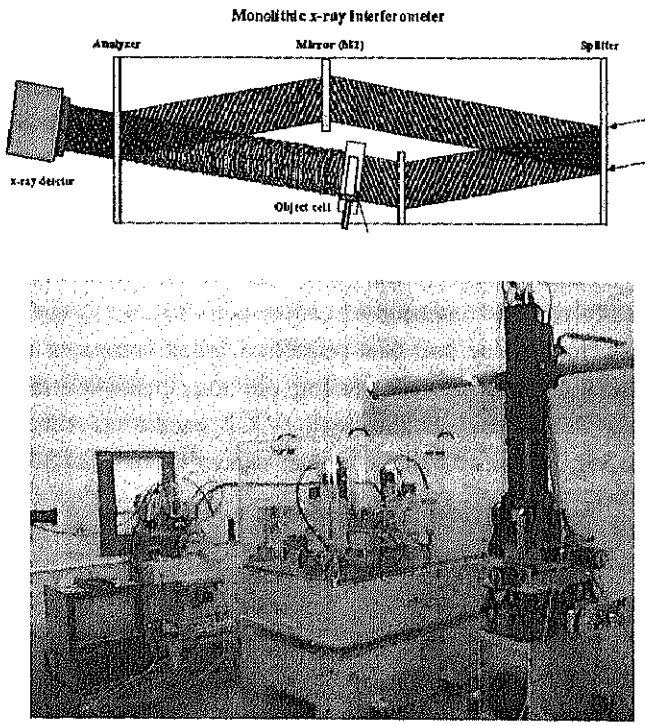

Fig.5 Schematic diagram and picture of phase-contrast x-ray system with monolithic x-ray interferometer.

Phase-contrast x-ray projection image (phase map)

Phase map which describes spatial distribution of the phase shift within a sample, cannot be obtained directly using the interferometer. The technique of phase-shift interferometry is used to generate phase map [18].

The phase map was obtained from several interference patterns (five in this experiment), which

were measured sequentially by changing the phase of the reference beam. Each interference pattern was acquired at 3sec exposure, and the total exposure time to obtain for a phase map was 15sec. The cell was inserted in a beam path between the mirror and the analyzer of the interferometer. The thickness of sample cell was 12mm.

Phase-contrast x-ray CT

Phase-contrast x-ray CT images mapped the variation of the refractive index. Since the x-ray beam was fixed, the specimens had to be rotated inside the cell filled with water. The total beam exposure time was 60sec/projection. The number of projections was 200 for 180 degrees. Phase-contrast x-ray CT images were reconstructed with a voxel size of 0.018mm.

Objects

Objects were rabbit and human cancers. For CT experiment, a 10mm in diameter column specimen was cut from rabbit liver because the photon flux of 17.7keV reaches to detector becomes small amounts due to huge absorption of thick object. For vessel imaging, physiological saline, which enhances the vascular contrast, was injected from the portal vein and whole blood in the liver was replaced.

Results and discussion

Phase-contrast x-ray CT

Phase-contrast x-ray CT of gallbladder cancer clearly revealed invasion of cancer cells to liver (Fig.6). Cancerous tissue had low refractive index compared to normal liver tissue, conforming previous phase-contrast x-ray CT results obtained with VX-2 cancer of rabbits [30,35], and with various human cancer tissues [32,33].

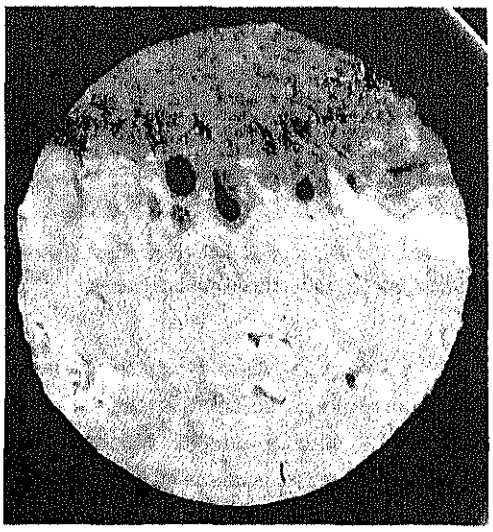

Fig.6 Phase-contrast x-ray CT image of gallbladder cancer. Diameter of sample is 10mm.

However, the very fine morphological structure of specimens that was smaller than 0.03mm could not be visualized by this phase-contrast x-ray CT.

Phase-contrast x-ray vessel imaging

Vessels over 0.03mm-diameter of excised rat liver clearly depicted by phase map after the injection of physiological saline (Fig.7). Usually in the absorption-contrast method, the iodine contrast agent having demerits such as high osmolarity, high viscosity and allergic reaction, is indispensable for vessel imaging, and x-ray exposure of 17times higher from the present phase map (113mR) was required to depict the vessel of 0.03mm-diameter [36]. Thus, the use of physiological saline for vessel imaging has significant merits because the side effect of the presently used iodine contrast agent is completely eliminated. In addition, the reduction of x-ray exposure becomes possible.

Fig.7 Phase map of hepatic vessel obtained by physiological saline.

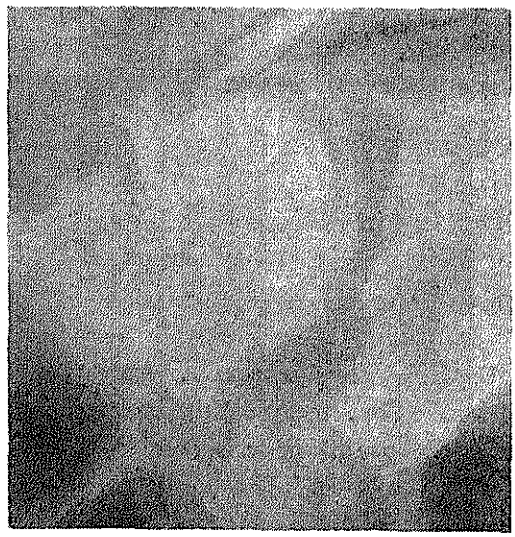

Fig.8 Phase map of breast cancer at 35keV x-ray energy.

Phase map of breast specimen

Clear phase map of breast specimens were obtained at 35keV x-ray energy, whereas imaging has not be succeeded at 17.7keV because the unwrapping could not be performed by the complex interference fringes. Phase map depicted micro-calcifications, spiculation, tumor extension and inner structure of cancer lesion clearly (Fig.8). In particular, soft tissue contrast within cancer, which could not be revealed by other phase-contrast techniques as diffraction-enhanced imaging [37,38], was significantly improved.

Present limitations and future plans

The current spatial resolution of our system is limited to about 0.03mm owing to the diffraction phenomenon within the crystal wafers in the analyzer [39]. To improve this spatial resolution, an interferometer with a thinner wafer for the analyzer is being planned.

In a monolithic x-ray interferometer, the maximum image size is limited by the diameter of silicon ingot. Therefore, a non-monolithic one, is currently being developed to obtain a large field of view of 100x100mm [40,41]. Using this interferometer, we are planning to perform phase-contrast x-ray mammography in vivo of the human breast.

4.CONCLUSIONS

FXCT is useful technique to analyze the functional information with high spatial resolution, whereas phase-contrast x-ray imaging enables to reveal the detailed morphological information such as cancer and vessel. Further the improvement of imaging system with high-speed data acquisition and much higher spatial resolution will give us new biological information.

Acknowledgement

We thank Mr. Kouzou Kobayashi for his preparation of experimental apparatus. This research was partially supported by Grant-In-Aid for Scientific Research (#12307018, #13470178) and for Special Coordination Funds from the Ministry of Education, Culture, Sports, Science and Technology, and was performed under the auspices of High Energy Accelerator Research Organization (99G124, 99S2-002).

References

1. Takeda T, et al. X-ray micro-computed tomography using synchrotron radiation. Edited by Kirkham N, Lemoine NR, Progress in Pathology. pp81-102, Greenwich Medical Media Ltd. UK, 2001

2. Takeda T, et al: New types of x-ray computed tomography with synchrotron radiation: fluorescent x-ray CT and phase-contrast x-ray CT with interferometer. Cellular & Molecular Biology 46, 2000, 1077-1088

3. Takeda T, et al. X-ray imaging with monochromatic snchrotron radiation. Med. Imag. Tech. 20 in press

4. Iida A, et al. Tracer element analysis by X-ray fluorescent. Edited by Ebashi S, Koch M, Rubenstein E. Handbook on Synchrotron Radiation. Vol 4 pp307-348 North-Holland, Elsevier Publisher, Amsterdam 1991

5. Boisseau P, et al. Fluorescence tomography using synchrotron radiation. Hyperfine Interactions 33, 1987, 283-292

6. Takeda T, et al: Fluorescent scanning x-ray tomography with synchrotron radiation. Rev. Sci. Instrum. 66, 1995, 1471-1473

7. Takeda T, et al. Fluorescent scanning x-ray tomographic image with monochromatic synchrotron x-ray. Med. Imag. Tech. 14, 1996, 183-194

8. Hogan JP, et al. Fluorescent computer tomography: A model for correction of X-ray absorption. IEEE Trans. Nucl. Sci. 38, 1991, 1721-1727

9. Takeda T, et al.: Fluorescent x-ray computed tomography with synchrotron radiation using fan collimator. SPIE 2708, 1996, 685-695

10. Rust GF, et al. X-ray fluorescent computed tomography with synchrotron radiation. IEEE Trans. Nucl. Sci. 45, 1998, 75-88

11. Takeda T, et al. Human thyroid specimen imaging by fluorescent x-ray computed tomography with synchrotron radiation. SPIE 3772, 1999, 258-267

12. Takeda T, et al. Iodine imaging in thyroid by fluorescent X-ray CT with 0.05 mm spatial resolution. Nucl. Instr. Meth. A467/468, 2001, 1318-1321

13.Takeda T, et al. Medical imaging by Fluorescent x-ray XT: Its preliminary clinical evaluation SPIE 4503, 2001, 299-309

14. Simionovici AS, et al. X-ray fluorescent microtomography: Experiment and reconstruction. SPIE 3772, 1999, 304-310

15. Yu Q, et al. Basic investigation of fluorescent x-ray computed tomography using synchrotron radiation for biomedical use. Med. Imag. Tech. 18, 2000, 805-816

16. Yu Q, et al. Preliminary experiment of fluorescent X-ray computed tomography to detect dual agents for biological study. J. Synchrotron Rad. 8, 2001, 1030-1034

17. Yuasa T, et al. Reconstruction method for fluorescent x-ray computed tomography by least-squares method using singular value decomposition. IEEE Trans. Nucl. Sci. 44, 1997, 54-62

18. Momose A, et al. Phase-contrast radiographs of

nonstained rat cerebellar specimen. Med. Phy. 22, 1995, 375-379
19. Takeda T, et al. Phase-contrast imaging with synchrotron x-rays for cancer lesion. Academic Radiol. 2, 1995, 799-803
20. Ando M, et al. An x-ray trichrome image 'Trinity': absorption, phase-interference and angle-resolved contrast. Jpn. J. Appl. Phys. 40, 1999, L298-301
21. Bonse U, et al. An X-ray interferometer. Appl. Phys. Lett. 6, 1965, 155-156
22. Davis TJ, et al. Phase-contrast imaging of weakly absorbing materials using hard X-rays. Nature 373, 1995, 595-598
23. Chapman D, et al. Diffraction enhanced x-ray imaging. Phys. Med. Biol. 42, 1997, 2015-2025
24. Snigirev A, et al. Phase contrast microimaging by coherent high energy synchrotron radiation. ESRF News Letter 24:23-25, 1995, Rev. Sci Instrum. 66, 1995, 5486-5492
25. Wilkins SW, et al. Phase-contrast imaging using polychromatic hard x rays. Nature 384, 1996, 335-338
26. Yagi N, et al. Refraction-enhanced x ray imaging of mouse lung using synchrotron radiation source. Med. Phys. 26, 1999, 2190-2193
27. Mori K, et al. First observation of small fractures on a human dried proximal phalanx by synchrotron x-ray interference radiography. Jpn. J. Appl. Phys. 38, 1999, L1339-1341
28. Hwu Y, et al. Coherence-enhanced synchrotron radiology: Refraction versus diffraction mechanisms. J. Appl. Phys. 86, 1999, 4613-4618
29. Momose A. Demonstration of phase-contrast X-ray computed tomography using an X-ray interferometer. Nucl. Instr. Meth. A352, 1995, 622-628
30. Momose A, et al. Phase-contrast x-ray computed tomography for observing biological soft tissue. Nature Med. 2, 1996, 473-475
31. Beckmann F, et al. X-ray microtomography using phase contrast for the investigation of organic matter. J Comput. Assist. Tomogr. 21, 1997, 539-553
32. Takeda T, et al. Phase-contrast x-ray CT image of breast tumor. J. Synchrotron Rad. 5, 1998, 1133-1135
33.Takeda T, et al. Human carcinoma: Early experience with phase-contrast x-ray CT image with synchrotron radiation: Comparative specimen study with optical microscopy. Radiology 214, 2000, 298-301
34. Takeda T, et al. Phase-contrast x-ray imaging with a large monolithic x-ray interferometer. J. Synchrotron Rad. 7, 2000, 280-282
35. Takeda T, et al. Phase-contrast x-ray computed tomography of non-formalin fixed biological objects. Nucl. Instrum. Meth.A467-468, 2001, 1322-1325
36. Takeda T, et al. Vessel imaging by interferometric phase-contrast x-ray technique. Circulation 105, 2002, 1708-1712
37. Arfelli F, et al. Mammography with synchrotron radiation: phase-detection techniques. Radiology 215, 2000, 286-293
38. Pisano ED, et al. Human breast cancer specimens: Diffraction-enhanced imaging with histological correlation -improved conspicuity of lesion detail compared with digital radiography. Radiology 214, 2000, 895-901
39. Hirano K, et al. Development of an x-ray interferometer for high-resolution phase-contrast x-ray imaging. Jpn. J. Appl. Phys. 38, 1999, L1556-1558
40. Yoneyama A, et al. Operation of a separated-type X-ray interferometer for phase-contrast imaging. Rev. Sci. Instrum. 70, 1999, 4582-4586
41. Yoneyama A, et al Large-area phase-contrast x-ray imaging system using a two-crystal x-ray interferometer. J Synchrotron Rad. submitted.